Mechanical Systems and Signal Processing 103 (2018) 352–367

Contents lists available at ScienceDirect

Mechanical Systems and Signal Processing

journal homepage: www.elsevier.com/locate/ymssp

Identification of walking human model using agent-based modelling

Erfan Shahabpoor [a,b,*], Aleksandar Pavic [c], Vitomir Racic [d,e]

[a] Department of Architecture and Civil Engineering, University of Bath, Claverton Down, Bath BA2 7AY, UK
[b] INSIGNEO Institute for In-Silico Medicine, Department of Civil & Structural Engineering, University of Sheffield, Sheffield S1 3JD, UK
[c] Vibration Engineering Section, College of Engineering, Mathematics and Physical Sciences, University of Exeter, UK
[d] Department of Civil and Environmental Engineering, Politecnico di Milano, Italy
[e] Department of Civil & Structural Engineering, University of Sheffield, UK

ARTICLE INFO

Article history:
Received 29 August 2016
Received in revised form 12 September 2017
Accepted 20 October 2017

Keywords:
Human-structure interaction
Vibration serviceability
Discrete traffic model
SDOF moving human model
FRF-based modal testing

ABSTRACT

The interaction of walking people with large vibrating structures, such as footbridges and floors, in the vertical direction is an important yet challenging phenomenon to describe mathematically. Several different models have been proposed in the literature to simulate interaction of *stationary* people with vibrating structures. However, the research on *moving* (walking) human models, explicitly identified for vibration serviceability assessment of civil structures, is still sparse. In this study, the results of a comprehensive set of FRF-based modal tests were used, in which, over a hundred test subjects walked in different group sizes and walking patterns on a test structure. An agent-based model was used to simulate discrete traffic-structure interactions. The occupied structure modal parameters found in tests were used to identify the parameters of the walking individual's single-degree-of-freedom (SDOF) mass-spring-damper model using 'reverse engineering' methodology. The analysis of the results suggested that the normal distribution with the average of $\mu = 2.85$Hz and standard deviation of $\sigma = 0.34$Hz can describe human SDOF model natural frequency. Similarly, the normal distribution with $\mu = 0.295$ and $\sigma = 0.047$ can describe the human model damping ratio. Compared to the previous studies, the agent-based modelling methodology proposed in this paper offers significant flexibility in simulating multi-pedestrian walking traffics, external forces and simulating different mechanisms of human-structure and human-environment interaction at the same time.

1. Introduction

Over the past three decades, investigations into a considerable number of vibration serviceability problems of structures [1,2], both in the vertical and horizontal directions, have highlighted the inability of the current design methods to reliably estimate the vibration response of structures to walking pedestrians. This is mainly due to the methods ignoring the natural *inter-* and *intra- subject variability* of people and their *interaction* with vibrating structures [2–5]. This is despite such interactions have been an integral part of the design process relating to vehicle-structure interaction for a long time [6,7]. The excessive lateral vibration of the London Millennium Bridge in 2000 caused a wave of research on the interaction of walking people with pedestrian structures in the lateral direction [8]. However, human-structure interaction (HSI) in the vertical

* Corresponding author at: Department of Architecture and Civil Engineering, University of Bath, Claverton Down, Bath BA2 7AY, United Kingdom.
E-mail address: e.shahabpoor@bath.ac.uk (E. Shahabpoor).

https://doi.org/10.1016/j.ymssp.2017.10.028
0888-3270/

direction during walking has been explored much less, is not understood well and consequently does not feature in key design guidelines [9–11]. However, the importance of HSI in the vertical direction is most recently demonstrated by Zivanovic et al. [11], Shahabpoor et al. [10] and Kasperski [12] based on experimental data collected from full-scale structures.

One of the key mechanisms of the HSI in the vertical direction is the effect of the human body on the dynamics of the structure over which the body moves. It is well known that the mass of a stationary human body accelerates when exposed to structural vibration and applies interaction force to the structure [13]. The same applies to the moving body, in which case *additional* ground reaction force (GRF) is created due to the base vibration. This force is super-imposed on the normal GRF, caused by acceleration and deceleration of the internally propelled human body and manifests itself as changes in the modal frequency (i.e. mass and/or stiffness) and damping of the empty structure. This is because such force has components proportional to the acceleration, velocity and displacement of the structure, as well as independent components [14].

In the past, several biodynamic models, such as a single degree of freedom (SDOF) mass-spring-damper model, were suggested to simulate the effects of walking humans on the structural vibrations in the vertical direction [15–21]. In most of these models, however, the human model parameters were adopted from the biomechanics literature and were not validated for the vibration serviceability assessment of civil structures. The works of Silva and Pimentel [16], Toso et al. [21] and Shahabpoor et al. [22] are the only examples to date known to the authors that propose a range of parameters for the SDOF walking human model in the context of the vibration serviceability of civil structures. Silva and Pimentel [16] suggested three empirical equations for mass (m), damping (c) and stiffness (k) of the SDOF human model by analysing the vertical walking force and measured vertical acceleration of the human trunk recorded at the pelvis (i.e. waist):

$$m = 97.082 + 0.275 \times M - 37.518 \times f_p \tag{1}$$

$$c = 29.041 \times m^{0.883} \tag{2}$$

$$k = 30351.744 - 50.261 \times c + 0.035 \times c^2 \tag{3}$$

In Eqs. (1)–(3), M [kg] is the total mass of the human body, f_p [Hz] is the pacing frequency and m [kg], c [Ns/m] and k [N/m] are the human SDOF model mass, damping and stiffness, respectively.

Toso et al. [21] used a similar methodology to calculate the spectral amplitudes of the first three harmonics of the vertical acceleration measured at the waist level of 35 test subjects. In addition, they calculated spectral amplitudes of the first three harmonics of the corresponding vertical GRF, which was also measured simultaneously with the acceleration of the pelvis. They used artificial neural network (ANN) to relate the biodynamic parameters to the pedestrians pacing rate and body mass:

$$m(f_p, M) = -231.34 + 3.69M + 154.06f_p - 1.97Mf_p + 0.005M^2 - 15.25f_p^2 \tag{4}$$

$$c(M, m) = -1115.69 + 92.56M - 108.94m + 2.91Mm - 1.33M^2 - 1.30m^2 \tag{5}$$

$$k(M,f_p) = 75601.45 - 1295.32M - 33786.75f_p + 506.44Mf_p + 3.59M^2 + 539.39f_p^2 \tag{6}$$

Both studies provided invaluable insights into the ranges of SDOF walking human parameters. However, they lack convincing experimental verification on real-world structures. The recorded acceleration of the pelvis was not transformed from the internal (i.e. local) coordinate frame of the measuring sensor to the Earth global frame, where the vertical axis is parallel to the gravity. Therefore, the recorded 'vertical' accelerations most likely contain some levels of error due to the rotation of the pelvis during walking [4,14]. Finally, common to all 'black box' approaches, the ANN used in Toso et al. study does not provide any physical insight on the obtained SDOF m, c and k parameters.

Shahabpoor et al. [22] used a comprehensive set of experimental data, measured on a full-scale post-tensioned concrete footbridge for different sizes of walking pedestrian traffics to identify parameters of a SDOF walking human model. A discrete multi-degree-of-freedom model of human–structure system was used to simulate the interaction of multi-pedestrian walking traffic with the vibrating structure. Each walking human was modelled using an SDOF MSD model. The structure was also modelled with an SDOF model representing a mode of its vibration. The analysis identified the range of 2.75–3.00 Hz for the natural frequency and 27.5–30% for the damping ratio of the SDOF model of a walking human, having a constant mass of 70 kg. The identification procedures used in this study modelled the time-varying location of walking pedestrians on the structure with an increasing level of detail and complexity. However, in all of these procedures the location of the walking human body on the structure was assumed to be 'stationary' during each time-step of the simulation selected to be sufficiently small. The effects of walking forces and shaker force (during forced FRF tests) were also assumed negligible.

To address these limitations, this paper utilises a very comprehensive set of multi-pedestrian walking traffic tests over a laboratory-based but realistic 15-tonne prototype footbridge structure. An *agent-based* traffic-structure model (ABM) was then used for simulation, where each individual and the relevant mode of the structure were both modelled using a SDOF mass-spring-damper model. The natural frequency and damping ratio of the walking human SDOF model were identified for each test in a way that the analytical frequency response function (FRF) of the occupied structure (OS) matched its experimental counterpart. Compared to the Shahabpoor et al. [22], the identification methodology proposed in this paper

(ABM) is a major step forward, taking into account the effects of walking forces and shaker force on the dynamic behaviour of the structure and making it possible to simulate 'moving' pedestrians realistically.

It needs to be mentioned that, only the HSI in the form of the effects of walking human body (modelled as a mass-spring-damper) on modal properties of the empty structure was studied in this research. Other HSI mechanisms, such as lock-in effects and synchronization, were not considered in this paper.

Section 2 of this paper presents a short introduction into agent-based modelling and its application to vibration serviceability assessment. A concise description of the two experimental campaigns and the data used for the analysis are presented in Section 3. In Section 4, the proposed identification procedures and the discrete ABM of the walking traffic-structure system are described in detail. Results of the analysis are presented in Section 5 in the form of the statistical distributions of the natural frequency and damping ratio of the walking human SDOF model. The conclusions are summarised in Section 6.

2. Agent-based modelling

An ABM, sometimes called an individual-based model (IBM), is a class of computational micro-scale models for simulating the actions and interactions of autonomous 'agents' to assess the overall system behaviour. Agents are the smallest elements of the system that interact with other parts of the system. Conceptually, ABM defines the behaviour of agents at the micro level and the macro behaviour of the system emerges from all the interactions between entities [23].

ABMs have been used widely in the simulation of crowd in the context of traffic routing and evacuations [24]. However, their application to vibration serviceability problems is very rare. To the best of the authors' knowledge, Carroll's work in 2013 [25] was the first attempt to use ABM in the field of vibration serviceability to simulate HSI. He used an inverted pendulum model of an individual walking person to model the *lateral* interaction of a multi-pedestrian traffic with a bridge structure. The hybrid interactions of pedestrians (i.e. with both the structure and other people in the vicinity) were considered in Carroll's simulations. This pioneering work shed light on the valuable potential of ABM in simulating a broader human-environment interaction (e.g. avoiding both stationary and moving obstacles). However, the potential for ABM modelling of HSI in the *vertical* direction has yet to be explored. This is important, as the HSI mechanism in the vertical direction is considerably different and a more widespread problem, than its counterpart in the lateral direction of the kind experienced by the London Millennium Bridge [26].

3. Experimental campaigns

The structure used in this study was a simply supported in-situ cast post-tensioned (PT) concrete full-scale prototype footbridge built for this purpose in the Light Structures Laboratory at the University of Sheffield. The structure rested on two knife-edge supports along its shorter edges, and behaved like a simply supported beam (Fig. 1). The total length of the footbridge was 11.2 m, including short 200 mm overhangs over the supports. Its rectangular cross section had a width of 2.0 m and a depth of 275 mm, and the structure weighed approximately 15 tonnes. Only the first two vertical bending modes of structure with modal frequencies 4.44 Hz and 16.8 Hz were considered relevant for this study. Although the natural frequency of the fundamental mode of the test structure (4.44 Hz) is beyond the reach of the frequency of normal walking, it is shown elsewhere to be highly susceptible to HSI [27].

Two series of tests (referred to as Series 'A' and 'B' here) were carried out on the full-scale prototype test footbridge of the University of Sheffield at different times, but with identical test setup. Each series comprised a set of FRF-based modal tests of the empty structure and the structure when a number of people were walking on it. Chirp signal was used to excite the structure in the frequency range of 3.5–5.5 Hz for the tests focused on the first mode (4.44 Hz), and 15–18 Hz for the tests focused on the second mode (16.8 Hz). An APS electro-dynamic shaker model 400, operated in the direct-drive mode, was connected to the slab from beneath, first at the mid-span (S1 in Fig. 1b) and then at the quarter-span (S2 in Fig. 1b), to achieve the highest possible excitation at the anti-node of mode 1 and 2, respectively. The point accelerance FRF was used for modal identification.

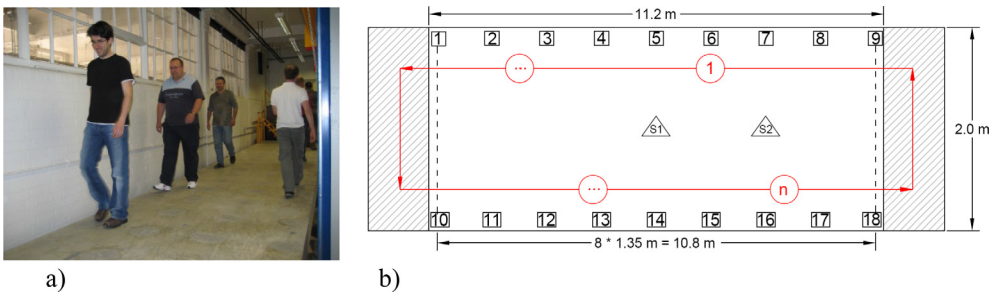

Fig. 1. Test structure (a) and a typical walking path on it (b) with 'n' pedestrians. S1 (mid-span) represents the location of the shaker and accelerometer for mode 1 tests and S2 (quarter-span) represents the location of the shaker and accelerometer for mode 2 tests.

In total, 8 tests focused on the first vibration mode and 3 tests focused on the second vibration mode were used for this study. In each test, a group of 2–15 people were walking along the full length of the structure and the modal properties of the occupied structure (coupled human-structure system) were estimated by curve-fitting the corresponding measured forced FRF. Full details of the test structure and the FRF-based test setup are presented in [22].

The identified modal properties of the empty structure are presented in Table 1 for both Series A and B tests. The analytically-calculated modal mass of 7128 kg, which is half of the total mass, was used for both modes assuming unity-scaled sinusoidal mode shapes. This was done to reduce the number of unknowns in the curve-fitting process of more or less noisy FRFs, as it will be shown later. A slight difference between empty structure modal properties is noticeable between Series A and B. This was attributed to the two series of tests being separated by approximately a year. Therefore, it is not surprising that 'nominally identical' modal tests produced slightly different estimates of modal properties, due to slightly different environmental conditions and long-term changes of structural properties.

3.1. Occupied structure tests

In each test, people were walking in a closed-loop path along the full length of the structure (Fig. 1). Test participants were asked to walk normally with their 'comfortable' speed, and they were free to pass each other. This was done so that each individual walked on the structure with a speed as close as possible to their normal walking speed recorded during treadmill test. This similarity was later validated by comparing the walking speed recorded on the structure using PeCo laser counters [22] and the corresponding treadmill speed for each pedestrian. Having established that walking speeds on the structure and treadmill are similar, it was further assumed that pacing frequency and step length of pedestrians during tests on the structure were equal to the corresponding values during treadmill tests. This assumption was necessary to be able to use treadmill-measured walking force signals for structural response simulation as individual walking force time histories could not be measured directly during the tests on the structure due to the high cost and lack of required equipment [4,28]. Although characteristics of the walking gait can be different when walking on a treadmill compared with walking on the structure, effects of these gait differences on dynamic properties of a walking human model were assumed negligible in this study. This assumption was made based on the characteristics of the walking force spectra which made it possible, as is justified below, to consider the walking excitation as narrow-band extraneous excitation uncorrelated with the excitation force, which was averaged out during experimental FRF estimation.

As the normal pacing frequencies of the test subjects (measured prior to the FRF tests) were between 1.60 Hz and 1.85 Hz, the frequency ranges of their 1st and 2nd walking force harmonics (1.60–1.85 Hz and 3.2–3.7 Hz, respectively) were below the frequency range of the modes of interest of the structure ($f_{es,1}$ = 4.44 Hz and $f_{es,2}$ = 16.8 Hz). As for the 3rd and 4th harmonics, their spectrum is characterised by low amplitude and wider energy spread compared with their 1st and 2nd harmonics counterparts. Therefore, the walking force spectra were expected to be low amplitude and quite flat around the frequencies of the modes of interest of the structure, especially as the number of people increased. To demonstrate this, Fig. 2 shows 5 spectra of the modal force due to walking (for mode 1 and mode 2) for Series A tests 1.1, 1.3, 1.4, 1.7 and 1.8 with 2, 4, 6, 10 and 15 pedestrians, respectively (Table 2). These are compared with the spectra for the corresponding shaker excitation. For each of the five tests, the modal walking force was calculated by combining the treadmill-measured walking force of each individual in the time domain assuming random time-shifts of their starts and by scaling them by the unity-scaled mode shape to take account of their exact location on the structure. It can be seen that, at around 4.44 Hz and 16.77 Hz, the walking force spectra are relatively flat over the relevant half-power bandwidth and have considerably lower amplitudes than the shaker excitation.

Hence, the characteristics of the walking force spectra due to the pedestrian traffic made it possible to consider the walking excitation as narrow-band extraneous excitation uncorrelated with the excitation force, which can be averaged out during experimental FRF estimation. Several strategies were used to minimise the effects of the unmeasured walking force excitation in the measured output. Chirp signal was used to excite the structure around its resonance. Chirp excitation, compared with a random excitation, allows the structure to build up the resonant response more strongly and, therefore, engages HSI mechanisms more effectively. The shaker was connected directly to the structure in a grounded mode to maximise the measured excitation energy transferred to the structure. These helped to achieve maximum signal (measured shaker force)

Table 1
Results of modal analysis of the empty structure.

Mode	FRF based						
#	Modal frequency f_{es}(Hz)	Modal damping ratio ζ_{es} (%)	Modal mass m_{es} (kg)	Modal damping coefficient c_{es} (N·s/m)	Modal stiffness k_{es} (N/m)	Maximum response a_{max} (m/s^2)	Response RMS a_{rms} (m/s^2)
1 (Series A)	4.44	0.6	7128	2386	5547×10^3	1.8782	0.3680
1 (Series B)	4.44	0.7	7128	2784	5547×10^3	2.6084	0.4826
2 (Series B)	16.77	0.4	7128	6009	$79{,}140 \times 10^3$	3.2123	0.5942

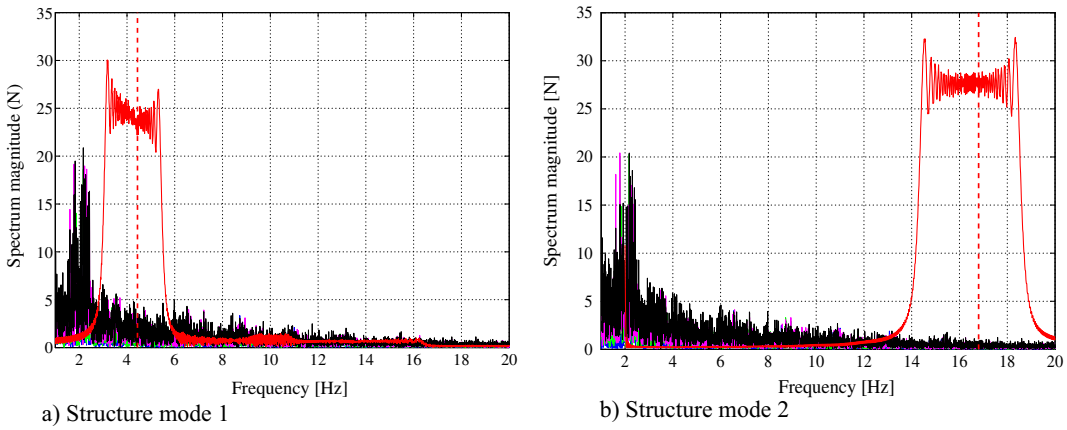

Fig. 2. Comparison of the spectra of the shaker force (red) and total modal traffic walking forces for Tests 1.1 (yellow), 1.3 (blue), 1.4 (green), 1.7 (purple) and 1.8 (black). Note that the walking force spectra have overlap. (For interpretation of the references to colour in this figure legend, the reader is referred to the web version of this article.)

Table 2
Modal properties of the occupied structure for different group sizes.

Test no.	Series	No. of pedestrians	Modal properties of the occupied structure					Structural response	
			f_{os} (Hz)	ζ_{os} (%)	m_{os} (kg)	c_{os} (N·s/m)	k_{os} (N/m)	a_{max} (m/s^2)	a_{rms} (m/s^2)
Mode 1 (Structure)									
1.1	A	2	4.443	1.00	7165	4000	5583×10^3	2.4361	0.4131
1.2	B	3	4.445	1.10	7183	4413	5603×10^3	1.7489	0.3018
1.3	A	4	4.450	1.28	7201	5154	5630×10^3	2.1755	0.3637
1.4	A	6	4.465	1.55	7238	6294	5696×10^3	1.8771	0.3311
1.5	B	6	4.465	1.65	7238	6701	5696×10^3	1.4882	0.2481
1.6	B	10	4.475	2.30	7311	9456	5780×10^3	1.1313	0.2050
1.7	A	10	4.476	2.10	7311	8635	5782×10^3	1.5876	0.2870
1.8	A	15	4.485	2.90	7402	12,140	5878×10^3	1.1251	0.2466
Mode 2 (Structure)									
2.1	B	3	16.900	0.55	7128	8326	$80{,}372 \times 10^3$	2.4059	0.4482
2.2	B	6	16.910	0.65	7128	9846	$80{,}468 \times 10^3$	2.2905	0.4234
2.3	B	10	16.935	0.75	7128	11,377	$80{,}708 \times 10^3$	2.1387	0.4023

to noise (part of the measured response due to unmeasured walking forces) ratio. This resulted in the RMS vibration response amplitudes being an order of magnitude higher for tests involving simultaneous action of the shaker and the walking people compared to the tests with people alone when the shaker was switched off. Also, the duration of the tests was prolonged to 15 min to enable sufficient averaging of the FRFs. This considerably reduced the effects of the uncorrelated excitation due to walking. Finally, the H1 FRF estimator was used to reduce the effects of the uncorrelated extraneous excitation due to unmeasured walking forces. The H1 estimator is obtained by dividing the Cross Spectral Density of the excitation-response signals by the Auto Spectral Density of the excitation signal and assumes that all of the measurement noise (unmeasured walking forces in this case) is in the response signal and can be averaged out [29]. Fig. 3 shows the beneficial effects of averaging in the case of the most demanding test (Test 1.8) involving 15 pedestrians. The fact that the FRFs became smooth and settled after only 3–4 averages indicates that the strategy employed worked well, yielding FRFs of reasonable quality that could be curve-fitted using linear models to estimate the modal parameters of the occupied structure [27].

3.2. Parameter identification

If the coupled human-structure dynamic system was behaving like a 2DOF (an SDOF for the human traffic and an SDOF for the structure) oscillator, two modes of vibration (i.e. two peaks in the FRF modulus plot) were expected in the experimental data [30]. However, the measured driving point accelerance FRFs feature only one apparent peak. This could be because the mode dominated by the human SDOF motion was highly damped, or it fell outside the frequency range displayed in the figures. Also, Matsumoto and Griffin [31] suggested that the FRF of the "global crowd" is expected to have a broad and low peak due to the natural difference between the dynamic behaviour of the bodies of individuals. Therefore, the curve fitting process used here was assuming an SDOF model representing the occupied structure.

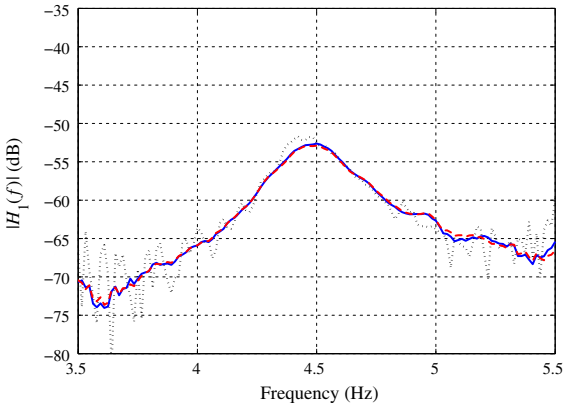

Fig. 3. Effects of averaging experimental FRFs for Test 1.8. (Dashed black: FRF corresponding to the first block; Blue: FRF after 6 averages; Dashed red: Final FRF after 15 averages). (For interpretation of the references to colour in this figure legend, the reader is referred to the web version of this article.)

The modal mass of the occupied structure was analytically estimated for each test. This was done by treating each pedestrian's body as an SDOF mass-spring-damper system attached to the structure. For each mode '*j*' of the structure, the modal mass of the occupied structure $m_{os,j}$ was estimated using Eq. (7) [29].

$$m_{os,j} = 0.5m_s + \sum_i m_{h,i}(\gamma_j \times \varphi_{i,j})^2; j = 1,2 \tag{7}$$

In this equation, $m_{h,i}$ is the total mass of human '*i*', m_s is the total mass of the structure, $\varphi_{i,j}$ is the structure unity-normalized mode '*j*' shape amplitude corresponding to the location of person '*i*' on the structure and γ_j is the ratio of the mode shape ordinate of the human DOF to the unity-normalized mode shape ordinate of the structure DOF for each mode '*j*'. A parametric study was carried out with varying human model natural frequency f_h and structure natural frequency f_s and it was found that γ_j is close to 0.85 for the first mode of structure (f_s = 4.44 Hz and $f_h \sim 2.85$ Hz) and is close to zero for the second mode of structure (f_s = 16.77 Hz and $f_h \sim 7$ Hz). Fig. 4 illustrates the 2DOF human-structure system when the very 'stiff' SDOF model of the *second mode* of structure (f_s = 16.77 Hz) interacts with the 'soft' SDOF model of human body (with $f_h \sim$2.85 Hz and ~7 Hz). In this case, around 16.8 Hz the mass of the human SDOF is almost not moving and is acting as restraint for the human spring stiffness and damper elements. This is why γ_j was assumed equal to zero and the mass of

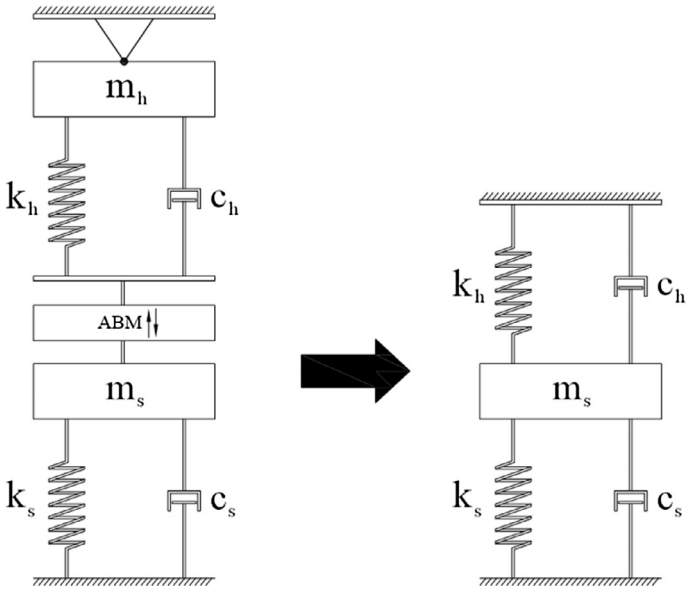

Fig. 4. The schematic of the restraint human DOF.

the occupied structure in Table 2 for Tests 2.1 – 2.3 was the same as the mass of the empty structure. However, the same table shows that the stiffness (k_{os}) and damping (c_{os}) coefficients pertinent to the occupied structure increase with more people on the structure, as expected.

The natural frequency f_{os} and damping ratio ζ_{os} of the occupied structure (OS) were initially estimated for each test using peak-picking and half-power bandwidth methods [32]. Then, for the calculated m_{os} parameters, empirical ranges of $0.95 \times f_{os,initial} \leq f_{os} \leq 1.05 \times f_{os,initial}$ and $0.75 \times \zeta_{os,initial} \leq \zeta_{os} \leq 1.25 \times \zeta_{os,initial}$ were defined around their initial values and used in the identification process. For each test, a pair of f_{os} and ζ_{os} parameters that resulted in the least square error fit of the experimental FRF magnitude curve (within frequency ranges of 3.5–5.5 Hz and 15–18 Hz for mode 1 and mode 2, respectively), assuming an SDOF model for FRF curve fitting, was identified and adopted for further analysis. For example, for 10 walking people Fig. 5 shows that the fit of both FRF amplitude and phase match well their experimental counterparts around resonance. This gives confidence that the methodology implemented here was robust and could be used for identifying the modal properties of various configurations of the occupied structure.

The occupied structure modal properties (f_{os}, m_{os} and ζ_{os}) are presented for all tests in Table 2. Comparing the occupied and empty structure modal properties (Table 1 and Table 2), the differences in the modal frequencies and, in particular, damping ratios, are noticeable. These changes were attributed to the effects of the HSI during walking. Hence, the identification methods developed in Section 4 use these observed effects to estimate the possible properties of the human SDOF model, which would yield the same observed effects for the two investigated modes of vibration of the occupied structure.

In Table 2, tests with 6 (Tests 1.4 and 1.5) and 10 (Tests 1.6 and 1.7) walking people were carried out with different test subjects and with a year time difference (Series A and B tests). In both cases, the two pairs of natural frequency f_{os} and damping ratio ζ_{os} of the occupied structure are almost identical, despite a year time gap and the fact that different human test subjects were used. Moreover, the trend of changes in f_{os} and ζ_{os}, observed in Series A and B tests are very similar. These observations provide confidence in the repeatability of the experimental results.

3.3. Identification assumptions

One of the key assumptions of the identification method used in this paper was that the presence of walking people on a structure did not affect its mode shape. This assumption was examined in [22]. It was also assumed that for a given number of people walking across the structure, the modal properties of the occupied structure m_{os}, c_{os} and k_{os} found from measured FRFs represent their *average* over the test duration. This assumption holds despite people's location changing continuously with time.

4. Identification of walking human model

The body of a walking human was assumed to behave as a linear SDOF mass-spring-damper system attached to a structure and being excited by the structure's vibration. The resulting human SDOF motion in turn generates a GRF that excites the structure in a 'feedback loop' process. This force is different from the walking GRF (generated by the human own locomotion) and is the result of subjecting the human body to a base excitation. The ABM used in this study uses this distinction between the two GRFs to simulate the interaction between the walking people and the vibrating structure.

Each pedestrian was simulated using an SDOF model. The interaction force between each walking individual and the structure could then be described as a sum of two forces (Fig. 6): (1) the walking GRF of that person on a stiff surface and (2) the GRF generated by the person's SDOF model excited by the structural vibration. This rationalisation was possible by assuming that the human body behaves linearly.

The same mass m_h, stiffness k_h and damping c_h parameters were used for all human SDOF models in each test. This was necessary to reach a unique solution in the optimization procedure. Although this assumption do not reflect the natural inter- and intra-subject variability of m_h, c_h, and k_h, it does not affect the validity of the identified m_h, c_h, and k_h parameters as an *average* value.

The structure was modelled as an SDOF system representing a single mode of the unoccupied structure at a time. It was assumed that behaviour of the structure is linear, hence its dynamic response can be decomposed into modal responses. In this way, the effects of the walking people on each mode of the structure can be calculated on a mode-by-mode basis, and then superimposed to get the total response of the occupied structure.

4.1. Agent-based model of discrete traffic – structure system

The ABM protocol used in this paper is adopted from the work of Grimm et al. [33]. Each pedestrian and the targeted mode of vibration of the structure were modelled as an agent, with dynamics formulated using an SDOF model. Fig. 7 describes the underlying structure of the ABM used to simulate each walking test. Each of the 'n' pedestrians, the target mode of the structure and the shaker excitation were simulated as an agent. These agents were interacting with each other in real time. The ABM controlled the interaction. A MATLAB code was used to carry out calculations simulating these interactions.

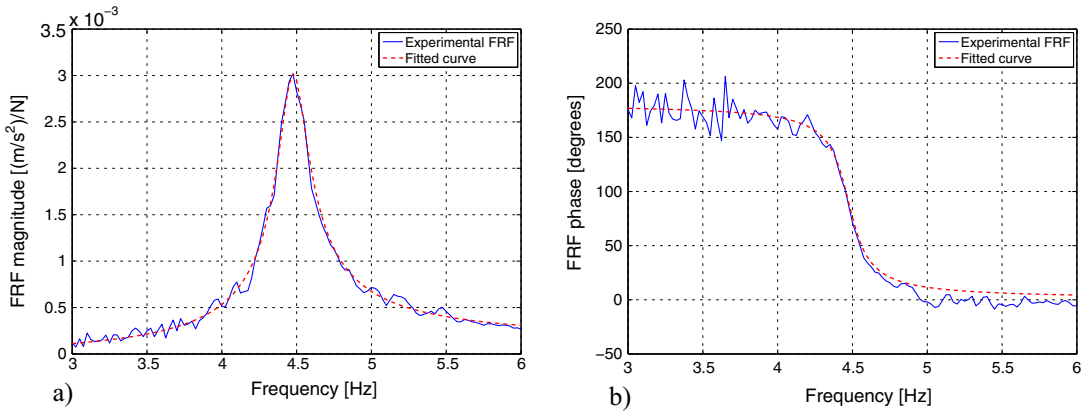

Fig. 5. The driving point experimental FRF amplitude (a) and phase (b) curves for accelerance and their analytical fit – Mode 1–10 pedestrians walking along the slab (Scenario S1).

The interactions of the people with obstacles in the pathway and with the surrounding environment were assumed negligible in this study, due to the controlled environment of the tests. However, the interaction of people with each other was introduced into the simulation to some extent by using the measured instantaneous location and speed of each human agent during the experiments, as elaborated in Section 3. Hence, no specific additional modelling of the human-human interaction was done. This significantly increased the accuracy of the simulations, since the associated errors of estimating human to human interactions were eliminated. It was also assumed that the structural vibrations did not affect the gait parameters (such as pacing frequency and length, speed etc.) of the pedestrians.

The following parameters were used in the ABM simulation:

- Structure SDOF model parameters m_{es}, c_{es} and k_{es}: they were set equal to the parameters of the target mode of the empty structure (Table 1).
- Human SDOF model parameters: m_h was set equal to the average mass of the pedestrians in the corresponding test. In each simulation, a pair of c_h and k_h were chosen from their predefined *initial ranges* as described in Section 4.2. The same parameters were used for all human models.
- Human GRF: the continuously measured vertical walking forces of each individual recorded using a treadmill were used repeatedly in the simulation for that person as their GRF.
- Location and walking speed of pedestrians: the measured time history of each pedestrian's location and walking speed in each test were used in the simulation.
- Time step: it was set to 0.01 s.
- Shaker force: the measured shaker force during each experiment was used in simulation.

In Eqs. (8)–(13) that follow, index *h*, *s* and *sh* represent human, structure and shaker, respectively. Moreover, *i* represents the current time step, n_{peds} is the total number of pedestrians and *j* index refers to the pedestrian number.

During the ABM simulation, the following sequence took place:

Initialisation: walking people SDOF models were placed at their initial positions on the structure (based on the corresponding test data). The structure was assumed to be at rest, so the structural response was set to zero for the first time step. The same assumption was made for the human SDOF models.

Then in each time step of the simulation:

I. Set the next time step (step '*i*').

$$t_i = t_{i-1} + \Delta t, \quad \Delta t = 0.01s \tag{8}$$

II. The walking people were moved to their new locations based on their location time histories recorded during the corresponding tests.

III. The acceleration response of the structure DOF from previous time-step ($\ddot{x}_s(t_{i-1})$) was transmitted to each SDOF human model as the base excitation. As shown in Fig. 8, the structural response that each person '*j*' feels was scaled by the mode shape amplitude $\Phi_s(L_{hj}(t_i))$ of the structure at the person's location $L_{hj}(t_i)$, as follows:

$$\ddot{x}_{s\to hj}(t_i) = \Phi_s(L_{hj}(t_i)) \times \ddot{x}_s(t_{i-1}) \tag{9}$$

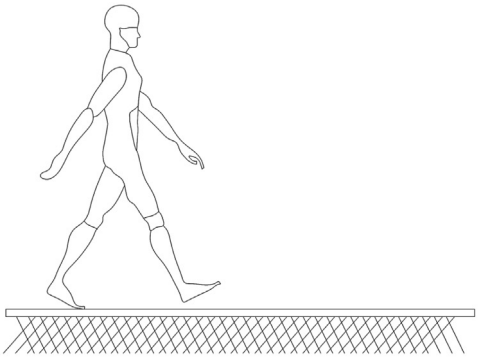

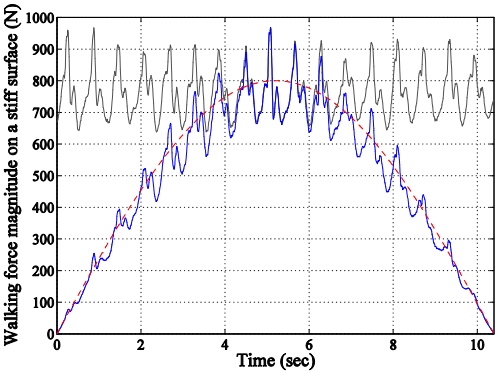

a) Walking force on stiff surface (grey) scaled to the first mode shape of a the test structure (blue)

+

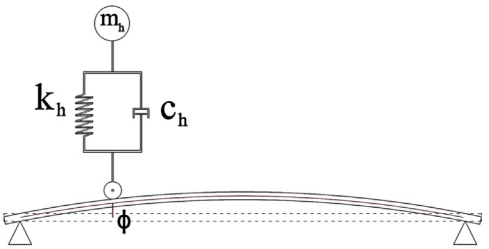

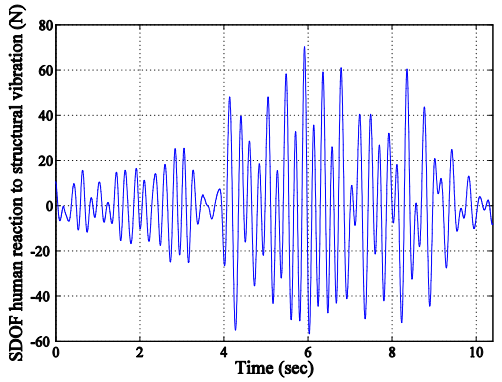

b) Force generated by mass of SDOF human model due to structural vibration

=

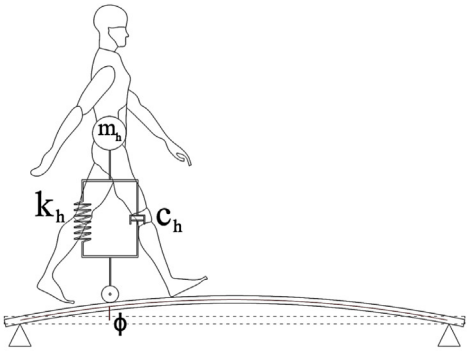

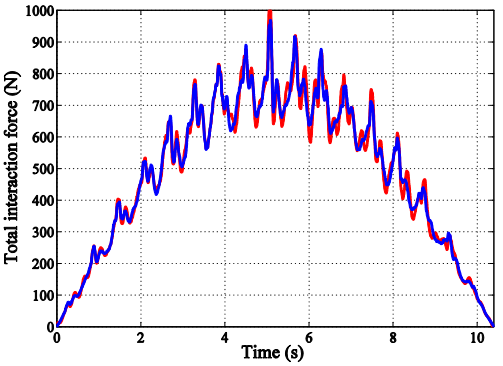

c) Total interaction force (red): combination of modal walking force (blue) and human response to structural vibration

Fig. 6. The interaction force composed of a modal walking force on a stiff surface and a human model response to structural vibrations. (For interpretation of the references to colour in this figure legend, the reader is referred to the web version of this article.)

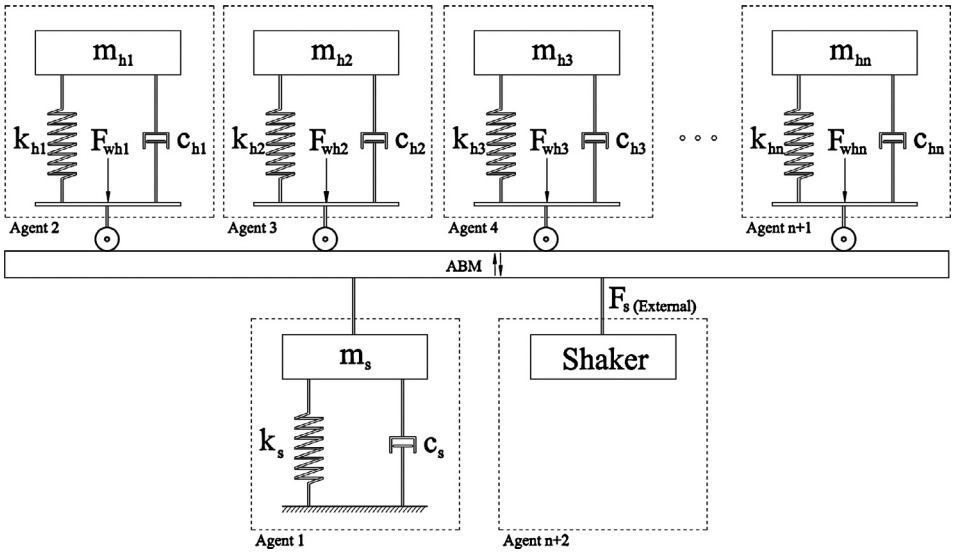

Fig. 7. Mechanical model of a walking people-structure system simulated by ABM.

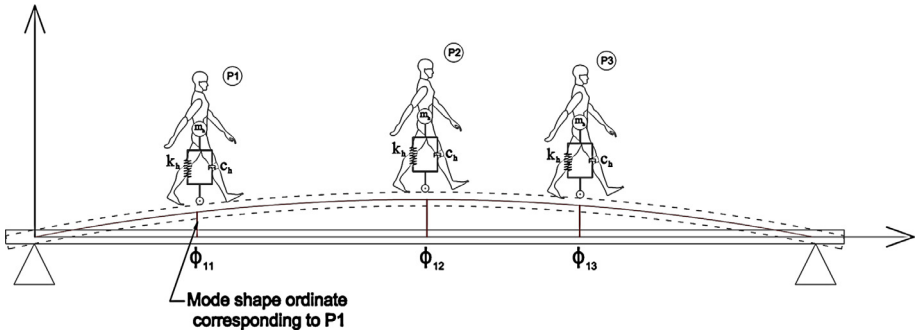

Fig. 8. Taking into account the modal effects of each pedestrian, based on their location on a structure.

IV. The response of each SDOF human model to its base excitation (Fig. 6b) was calculated using Newmark integration method [29]. This was done by taking into account the displacement and velocity of each human SDOF model from the previous time step as initial conditions for the current step, using the following equation of motion due to base excitation:

$$m_{hj}\ddot{x}_{hj}(t_i) + c_{hj}[\dot{x}_{hj}(t_i) - \dot{x}_{s\to hj}(t_i)] + k_{hj}[x_{hj}(t_i) - x_{s\to hj}(t_i)] = 0 \quad (10)$$

V. The interaction force $F_{int-hj}(t_i)$ (Fig. 6c) was calculated for each person by summing its walking force $F_{whj}(t_i)$ (recorded on a stiff surface using an instrumented treadmill) and its SDOF reaction to the base excitation ($m_{hj}\ddot{x}_{hj}(t_i)$), as follows:

$$F_{int-hj}(t_i) = F_{whj}(t_i) + m_{hj}\ddot{x}_{hj}(t_i) \quad (11)$$

VI. The interaction forces of all pedestrians and the experimentally-measured shaker force ($F_{sh}(t_i)$) were applied to the structure at their corresponding current locations (scaled by the structure mode shape based on pedestrians/shaker location at this time-step). As the shaker acts at an antinode of the relevant unity-scaled mode of the unoccupied structure, its mode shape-scaling factor is 1.0. The total force exciting the structure $F_{h+sh\to s}(t_i)$ can therefore be calculated as:

$$F_{h+sh\to s}(t_i) = 1 \times F_{sh}(t_i) + \sum_{j=1}^{n_{ped}} (\Phi_s(L_{hj}(t_i)) \times F_{int-hj}(t_i)) \quad (12)$$

VII. The response of the structure SDOF model was then calculated for the applied forces using Newmark integration method [29], by taking into account the displacement and velocity of the structure SDOF model from the previous time step, as initial condition for the current time-step:

$$m_s\ddot{x}_s(t_i) + c_s\dot{x}_s(t_i) + k_s x_s(t_i) = F_{h+sh\to s}(t_i) \quad (13)$$

VIII. The process was repeated using the newly calculated $\ddot{x}_s(t_i)$, starting from 'I' until the last time-step of the simulation.

It is worth mentioning that, using the structural response from the previous step would introduce a delay in the analysis. The effects of this delay can be minimized by reducing the simulation time-step. For the human traffic-structure system in this study, it was found that using 0.01 s time-step, results of the ABM and the conventional multiple degree of freedom (MDOF) formulation are almost identical.

4.2. Identification procedure

The identification procedure developed for this study was based on an iterative approach. Initial ranges of 1–12 Hz with 0.05 Hz steps for f_h and 5–50% with 2.5% steps for ζ_h were selected to model the walking human SDOF ('h' subscript is used instead of h_1, h_2, h_3, etc. here to refer generally to any participant). These ranges were selected based on the values suggested in the literature [34,35,36] and the recent independent study done by Silva and Pimentel [16] on walking people.

The ABM described in Section 4.1 was used to simulate each test and to calculate the occupied structure response at the anti-node of the target mode. This acceleration response and the corresponding shaker force were used to calculate the analytical (as opposed to experimentally measured) point accelerance FRF of the occupied structure. Strictly speaking, inclusion of treadmill-measured vertical GRFs was not necessary and pretty much the same ABM-simulated FRFs would have been obtained if all GRFs were assumed to be zero. However, they have been included for completeness of the work and as additional proof that typical GRFs are uncorrelated with the shaker excitation when calculating FRFs. Also, the ABM presented is a viable simulation procedure to calculate structural vibration response in the vertical direction which takes into account significant HSI from groups of people when their individual GRFs, SDOF body properties and locations are known or assumed.

These ABM-calculated FRFs were curve-fitted using the same SDOF-based procedure as for the experimental FRFs to find the occupied structure f_{os}, m_{os} and ζ_{os}. These parameters and the peak point accelerance FRF magnitude (a_{FRF}) were then compared with their experimental counterparts and the corresponding errors were calculated. This process was repeated for all pairs of f_h and ζ_h in each test. The same pair of f_h and ζ_h values was used in each simulation for all pedestrians to reduce the number of combinations needing analysis and make the results simpler to interpret. Mass of the human model m_h was assumed equal to the average mass of participants in the corresponding test. The empty structure modal properties presented in Table 1 were used for m_{es}, k_{es} and c_{es}.

An empirical series of maximum acceptable errors were defined for the estimated f_{os}, m_{os}, ζ_{os} and a_{FRF}. These were 0.01 Hz for f_{os}, 250 kg for m_{os}, 1% error for ζ_{os} and 20% error for a_{FRF}. For each test, there were several pairs of f_h and ζ_h yielding errors lower than the maximum acceptable. Therefore, ranges of f_h and ζ_h values were identified that predict f_{os}, m_{os}, ζ_{os} and a_{FRF} with errors less than the maximum values. These ranges are referred to as *test-verified* ranges in the rest of this study. For example, Fig. 9 shows a typical over-plot of occupied structure FRFs corresponding to these test-verified f_h and ζ_h ranges for test 1.5. It can be seen that any combination of f_h and ζ_h between their minimum and maximum values given for Test 1.5 in Table 3 produces an FRF (grey curves), which is very close to the measured FRF, with the error of a_{FRF}, relative to the measured FRF peak, well below the 20% maximum (Fig. 9b).

The measured and simulated acceleration response of the structure at mid-span are also compared in time-domain for Test 1.5 in Fig. 10. The pair of f_h and ζ_h values that predict f_{os}, m_{os}, ζ_{os} and a_{FRF} in Test 1.5 with minimum error is used in ABM to simulate the structural response. As it can be seen in Fig. 10b, the amplitude of the measured and simulated acceleration response match well statistically.

In the next step, the test-verified ranges of f_h and ζ_h were combined for all tests (for each mode separately) and a common range of f_h and ζ_h across all tests was found (Fig. 11 grey bars). This ensures that if any combination of f_h and ζ_h, selected from these common ranges was used to simulate people in any of the tests, the predicted f_{os}, ζ_{os} and a_{FRF} would be within the acceptable error margins previously defined.

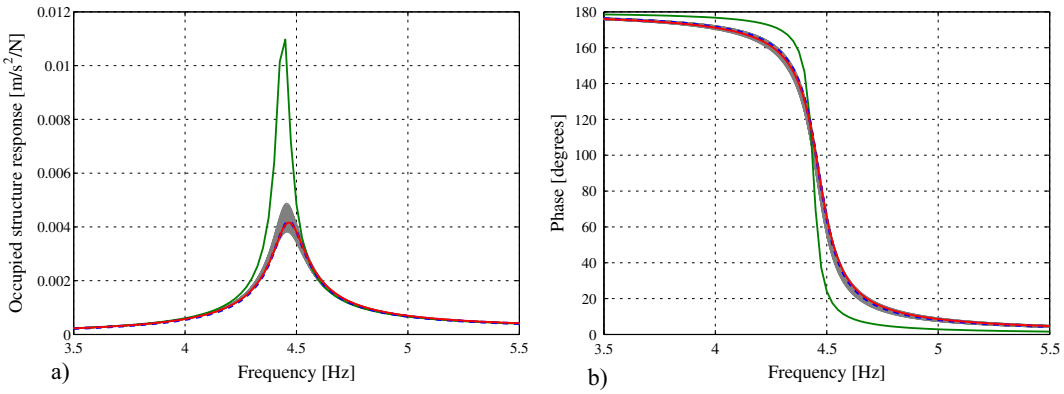

Fig. 9. A typical over plot of empty (green), experimental (red) and acceptable analytical occupied structure FRFs (grey) magnitude (a) and phase (b) – Test No 1.5 – (6 pedestrians). (For interpretation of the references to colour in this figure legend, the reader is referred to the web version of this article.)

Table 3
Test-verified ranges of SDOF human model parameters.

Test No.	No. of pedestrians	Average m_h (kg)	Acceptable ranges of SDOF human model parameters				
			f_h (Hz)		m_h (kg)	ζ_h (%)	
			Min	Max		Min	Max
Mode 1							
1.1	2	55	2.50	3.50	55	20.0	40.0
1.2	3	70	2.75	3.50	70	20.0	40.0
1.3	4	55	2.50	3.50	55	20.0	37.5
1.4	6	55	2.75	3.50	55	22.5	37.5
1.5	6	70	2.25	3.00	70	25.0	40.0
1.6	10	70	2.75	3.00	70	22.5	30.0
1.7	10	60	2.75	3.50	60	22.5	37.5
1.8	15	70	2.75	3.25	70	27.5	37.5
Mode 2							
2.1	3	80	6.5	9.0	80	10.0	17.5
2.2	6	70	6.0	8.0	70	10.0	22.5
2.3	10	70	6.0	7.5	70	10.0	22.5

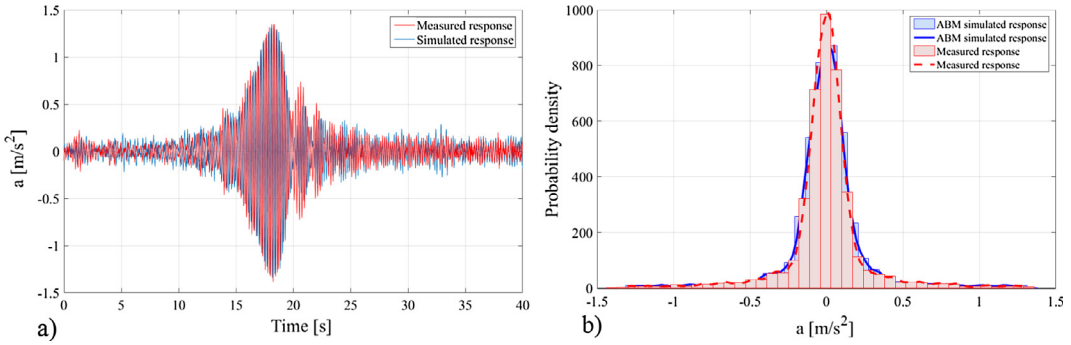

Fig. 10. Comparison of the measured (red) and estimated (blue) mid-span acceleration response time histories (a) and response amplitude histograms (b) – Test No 1.5 – (6 pedestrians). (For interpretation of the references to colour in this figure legend, the reader is referred to the web version of this article.)

5. Results

The test-verified ranges of the human model parameters f_h and ζ_h are presented in Table 3 and Fig. 11. As it can be seen, the ranges of f_h and ζ_h are different for mode 1 and 2 of the structure. This might be because the human body is not in reality an SDOF but an MDOF system. As such, a different mode of the walking human body is predominantly excited around a different frequency of the structural mode. A structural mode around 16.8 Hz predominantly engages a human mode, having natural frequency around 7 Hz rather than below 3 Hz. Detailed study of this interesting observation needs more similar experiments on different types of structures, and is beyond the scope of this paper. It should be noted here that in deriving values presented in Table 3 it was assumed that the mass of the human SDOF is the same as the physical mass of the whole of the human body. This was done to simplify estimation of the human SDOF parameters and create a model which is easy to use in practice. However, the mass of the human SDOF could have been treated as an uncertain modelling parameter as well, most likely resulting in slightly lower values of m_h and higher value of k_h to preserve the f_h found. However, it is unlikely that this consideration would have changed significantly the overall FRF simulation results as it would yield the combined human-structure FRFs which are of similar shape as those identified following the process described in this paper.

For each of modes 1 and 2, a range of f_h and ζ_h parameters was found that is common in all tests (Fig. 11 – grey bars). These *common ranges* of f_h and ζ_h were found to be 2.75–3.00 Hz and 27.5–30%, respectively, for the first mode of structural vibration (Fig. 11a and b – grey bars). In other words, any value of f_h between 2.75 and 3.00 Hz and ζ_h between 27.5% and 30% can simulate the effects of HSI in all mode 1 tests within the specified error band. For the second mode, the common ranges of f_h and ζ_h were found to be 6.5–7.5 Hz and 10–17.5%, respectively (Fig. 11c and d – grey bars).

A parametric study was carried out to analyse the accuracy of the estimated occupied structure parameters and the response when using f_h and ζ_h selected from their common ranges. Fig. 12 presents the errors associated with the estimated f_{os}, ζ_{os} and a_{FRF} (compared to their corresponding experimental values for mode 1 of the structure) when using any arbitrary combination of f_h and ζ_h selected from their common ranges. These errors were averaged over all eight tests pertinent to the first mode for each pair of f_h and ζ_h. Based on this figure, the maximum errors expected in the estimated f_{os}, ζ_{os} and a_{FRF} are 0.006 Hz (<0.01 Hz), 0.33% (<1%) and 9.8% (<20%) of the experimental FRF peak, respectively, which are considerably less than the assumed initial maximum acceptable errors used for the simulations.

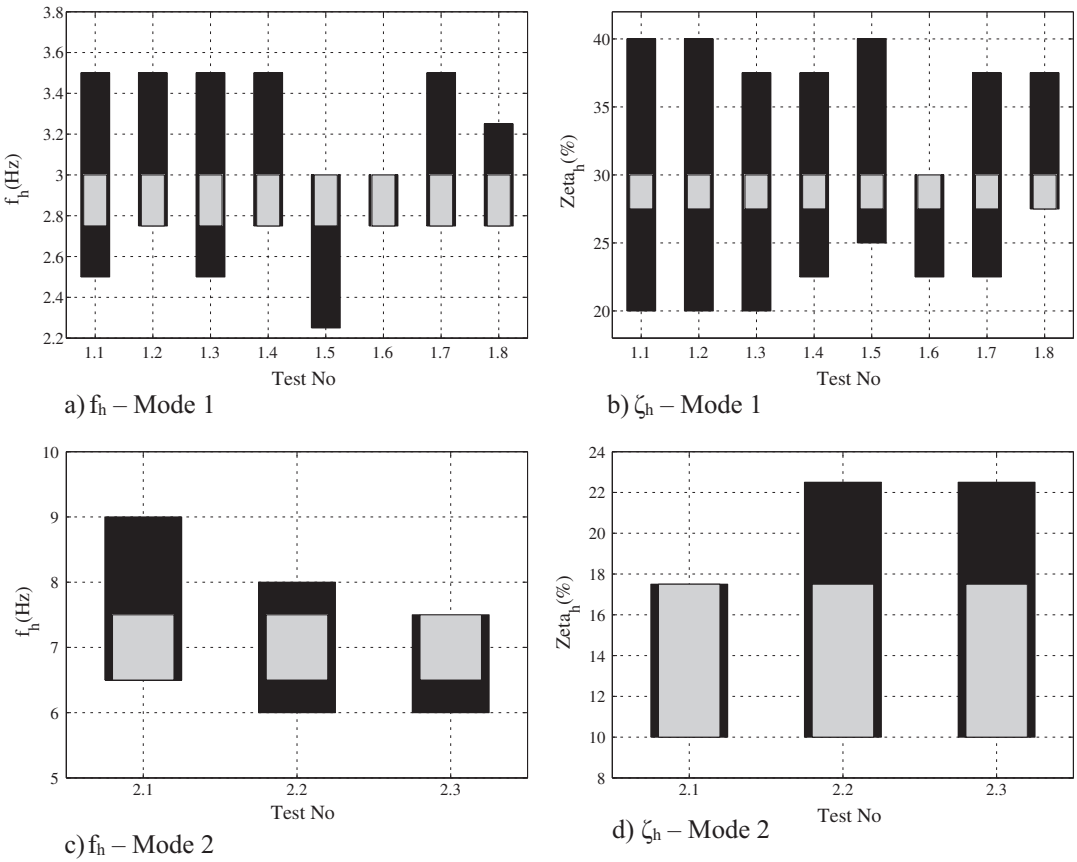

Fig. 11. Test-verified ranges of f_h and ζ_h found in different tests (black bars) and their common ranges (grey bars).

In the next step, the entire values in the test-verified ranges of f_h and ζ_h of all the eight tests related to mode 1 of the structure (Table 3) were combined and plotted in the form of f_h and ζ_h histograms (Fig. 13). A statistical distribution was then fitted empirically to each of these histograms. As it can be observed in Fig. 13, normal distribution was found to describe best the distribution of f_h and ζ_h. The mean μ and standard deviation σ of the suggested normal distributions were estimated using maximum likelihood method [37], as follows:

- μ = 2.85 Hz and σ = 0.34 Hz for f_h, and
- μ = 0.295 and σ = 0.047 for ζ_h.

These results are in line and comparable with the SDOF walking human model parameters suggested by Silva and Pimentel [16], determined independently by an entirely different procedure. For example, for human mass equal to 70 kg and 1.8 Hz mean pacing frequency, their model predicts f_h = 2.64 Hz and ζ_h = 0.55. While the natural frequency of the human body is very close to that found in the present study, Silva and Pimentel predicted higher human body damping, which anyway is a notoriously difficult parameter to estimate.

The results of this study are also closely in line with the results presented by Shahabpoor et al. [22]. Although both studies used a similar set of experimental data, they utilised fundamentally different approaches to simulate HSI. The Shahabpoor et al. [22] identified the occupied structure modal properties using eigenvalue extraction of the equation of motion of the MDOF pedestrian-structure system. While this study simulates numerically the forces walking pedestrians (agents) and the structure apply on each other to find the structural response. This response was then used to estimate the modal properties of the occupied structure. Regardless of this critical difference, similarity of the findings provides confidence in the validity of the identified parameters of the walking human model.

Similar ranges of f_h and ζ_h to the corresponding ranges identified in this paper, were used in a response simulation method proposed by Shahabpoor et al. [38] to estimate the structural response of the Podgorica footbridge in Montenegro under real-life walking traffic load. The estimated responses were reported to closely match the measured responses which again provides assurance in the validity of the identified parameters of the walking human model for a real-would structure and walking traffic.

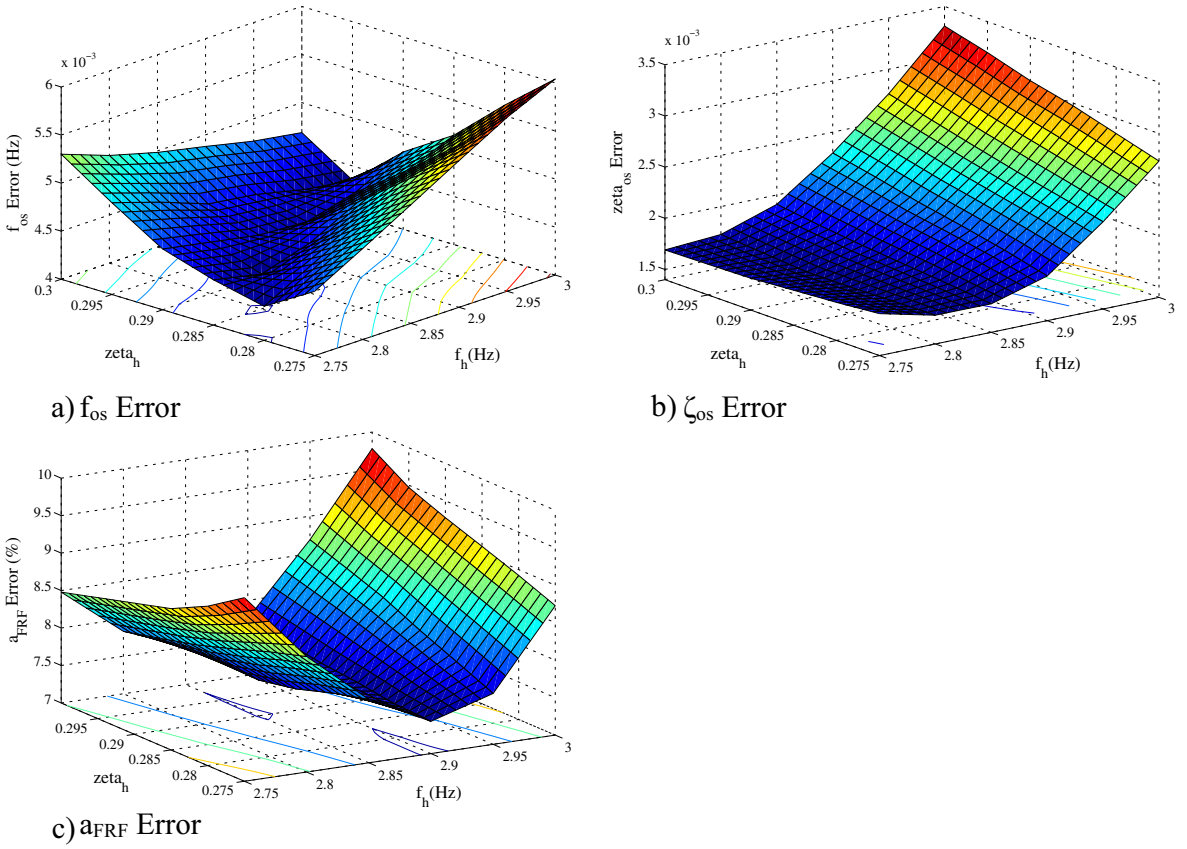

Fig. 12. Expected errors in occupied structure natural frequency f_{os}, damping ratio ζ_{os} and peak FRF magnitude a_{FRF} for the common ranges of human model parameters –Mode 1.

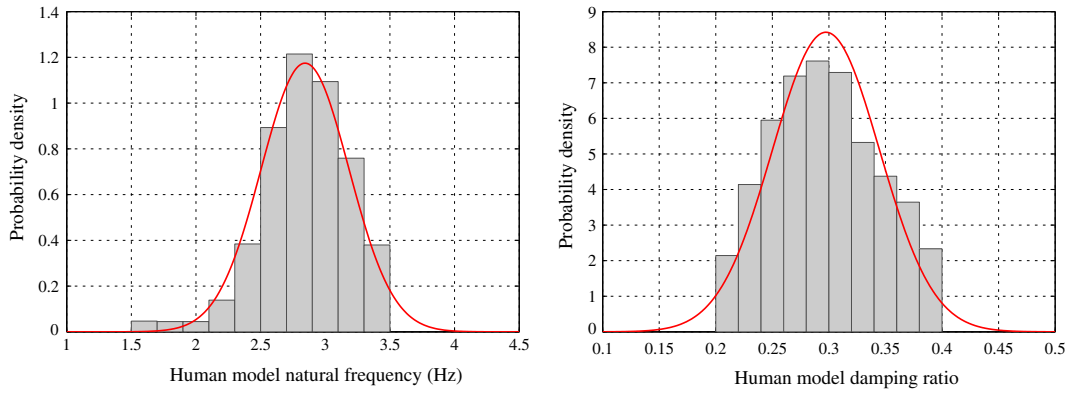

a) Normal distribution of natural frequency of human SDOF model f_h - μ=2.85 Hz and σ= 0.34 Hz

b) Normal distribution of damping ratio of human SDOF model ζ_h - μ=0.295 and σ= 0.047

Fig. 13. Probability density function of human SDOF model natural frequency (a) and damping ratio (b).

6. Summary and conclusions

The present work utilised comprehensive and rare traffic-structure experimental data to identify the mass, stiffness and damping parameters of an SDOF walking human model. A discrete agent-based model of the human traffic-structure system was used to simulate the walking tests. A linear SDOF mass-spring damper model was assumed to represent the dynamics of

a walking human. In FRF-based modal tests carried out on the occupied structure, it was further assumed that the pedestrian walking force on a rigid surface can be considered as uncorrelated random extraneous excitation - the effects of which can be averaged out using an H1 FRF estimator.

The key results of the study are:

- Normal distributions with a mean value of $\mu = 2.85$ Hz and a standard deviation of $\sigma = 0.34$ Hz, and $\mu = 0.295$ and $\sigma = 0.047$ can describe human model natural frequency f_h and damping ratio ζ_h, respectively.
- The difference between SDOF human model parameters found for modes 1 and 2 of the structure indicate that a moving human body is an MDOF system, which full identification following this methodology is still an unsolved research challenge in the context of moving pedestrians and vibration serviceability.
- The design of experiments used in this research can serve as a benchmark for data collection for other multi-pedestrian HSI studies in the future.
- The agent-based model used in this study demonstrates its great potential for reliable simulations of the multi-pedestrian – structure interaction in the vertical direction. This includes challenging aspects, such as uneven pedestrian flow and negotiating obstacles.

The comprehensive experimental data set, the detailed simulation process and the outputs consistent with the previous findings of other researchers provide confidence in the results. However, key limitations of this study were: (1) using partially identified SDOF model with its mass assumed for a walking human, (2) experimental data available for only one structure, and (3) unmeasured actual interaction forces between the pedestrians and the vibrating structure. Furthermore, the effects of walking load parameters such as walking speed, pacing rate, etc. on human model parameters are not studied in this paper.

Future research on the HSI in the vertical direction can build on the findings of this study and expand the suggested methodology with a fully identified MDOF human model and different real-life structures.

Acknowledgements

The authors acknowledge the financial support, which came from the University of Sheffield doctoral scholarship for Dr Shahabpoor and the UK Engineering and Physical Sciences Research Council (EPSRC) for the following research grants:

- Platform Grant EP/G061130/2 (Dynamic performance of large civil engineering structures: an integrated approach to management, design and assessment),
- Standard Grant EP/I029567/1 (Synchronisation in dynamic loading due to multiple pedestrians and occupants of vibration-sensitive structures), and
- Frontier Engineering Grant EP/K03877X/1 (Modelling complex and partially identified engineering problems: Application to the individualised multiscale simulation of the musculoskeletal system).

References

[1] R.L. Pimentel, A. Pavic, P. Waldron, Evaluation of design requirements for footbridges excited by vertical forces from walking, Can. J. Civil. Eng. 28 (5) (2001) 769–777, https://doi.org/10.1139/l01-036.
[2] S. Živanović, A. Pavic, E.T. Ingolfsson, Modelling spatially unrestricted pedestrian traffic on footbridges, J. Struct. Eng. 136 (10) (2010) 1296–1308.
[3] M. Kasperski, C. Sahnaci, Serviceability of pedestrian structures, in: Proceedings of the 25th International Modal Analysis Conference, Orlando, Florida, 2007, pp. 774–798.
[4] V. Racic, A. Pavic, J.M.W. Brownjohn, Experimental identification and analytical modelling of human walking forces: literature review, J. Sound Vib. 326 (2009) 1–49.
[5] E. Shahabpoor, A. Pavić, Comparative evaluation of current pedestrian traffic models on structures, in: Conference Proceedings of the Society for Experimental Mechanics Series, vol. 26, 2012. p. 41–52.
[6] Y.B. Yang, C.W. Lin, Vehicle–bridge interaction dynamics and potential applications, J. Sound Vib. 284 (2005) 205–226.
[7] S.G.M. Neves, A.F.M. Azevedo, R. Calçada, A direct method for analysing the vertical vehicle–structure interaction, Eng. Struct. 34 (2012) 414–420.
[8] A. Fitzpatrick, P. Dallard, S. le Bourva, A. Low, R. Ridsill Smith, M. Willford, Linking London: The Millennium Bridge, The Royal Academy of Engineering, London, 2001.
[9] S. Živanović, A. Pavic, Probabilistic modelling of walking excitation for building floors, J. Perform. Construct. Facil. 23 (3) (2009) 132–143.
[10] E. Shahabpoor, A. Pavić, V. Racic, Using MSD model to simulate human-structure interaction during walking, in: Conference Proceedings of the Society for Experimental Mechanics Series, 2013.
[11] S. Zivanovic, I.M. Diaz, A. Pavic, Influence of Walking and Standing Crowds on Structural Dynamic Properties, IMAC-XXVII, Orlando, Florida, USA, 2009.
[12] M. Kasperski, Damping Induced by Pedestrians, 9th EURODYN, Porto, Portugal, 2014.
[13] M. Griffin, Handbook of Human Vibration, Academic Press, London, 1990.
[14] V. Racic, J.M.W. Brownjohn, A. Pavic, Reproduction and application of human bouncing and jumping forces from visual marker data, J. Sound Vib. 329 (2010) 3397–3416.
[15] P.J. Archbold, J. Keogh, C. Caprani, P. Fanning, A parametric study of pedestrian vertical force models for dynamic analysis of footbridges, in: Proceeding of Experimental Vibration Analysis for Civil Engineering Structures Conference EVACES, 2011.
[16] F.T. Silva, R.L. Pimentel, Biodynamic walking model for vibration serviceability of footbridges in vertical direction, in: Proceeding of the 8th International Conference on Structural Dynamics (Eurodyn), 2011, pp. 1090–1096.

[17] F.T. Silva, H.M. Brito, R.L. Pimentel, Modeling of crowd load in vertical direction using biodynamic model for pedestrians crossing footbridges, Can. J. Civ. Eng. 40 (2013) 1196–1204, https://doi.org/10.1139/cjce-2011-0587.
[18] C.C. Caprani, J. Keogh, P. Archbold, P. Fanning, Characteristic vertical response of a footbridge due to crowd loading, in: Proceeding of the 8th International Conference on Structural Dynamics (Eurodyn), 2011, pp. 978–985.
[19] J.F. Jiménez Alonso, A. Sáez, A direct pedestrian-structure interaction model to characterize the human induced vibrations on slender footbridges, Informes de la Construcción 66 (EXTRA1) (2014) m007, https://doi.org/10.3989/ic.13.110.
[20] M. Zhang, C.T. Georgakis, W. Qu, J. Chen, SMD Model Parameters of Pedestrians for Vertical Human-Structure Interaction, IMAC XXXIII, Orlando, Florida, USA, 2015.
[21] M.A. Toso, H.M. Gomes, F.T. Silva, R.L. Pimentel, Experimentally fitted biodynamic models for pedestrian–structure interaction in walking situations, Mech. Syst. Signal Process. 72–73 (2016) 590–606.
[22] E. Shahabpoor, A. Pavić, V. Racic, Identification of mass–spring–damper model of walking humans, Structures 5 (2016) 233–246.
[23] M.W. Macy, R. Willer, From factors to actors: computational sociology and agent-based modeling, Annu. Sociol. Rev. 28 (2002) 143–166.
[24] X. Zheng, T. Zhong, M. Liu, Modelling crowd evacuation of a building based on seven methodological approaches, Build. Environ. 44 (3) (2009) 437–445, https://doi.org/10.1016/j.buildenv.2008.04.002.
[25] S.P. Carroll, Crowd-Induced Lateral Bridge Vibration. (PhD thesis), University of Nottingham, 2013
[26] P. Dallard, A.J. Fitzpatrick, A. Flint, S. Le Bourva, A. Low, R.M. Ridsdill Smith, M. Willford, The London millennium footbridge, Struct. Eng. 79 (22) (2001).
[27] E. Shahabpoor, A. Pavic, V. Racic, S. Zivanovic, Effect of group walking traffic on dynamic properties of pedestrian structures, J. Sound Vib. 387 (2017) 207–225, https://doi.org/10.1016/j.jsv.2016.10.017.
[28] V. Racic, A. Pavic, J.M.W. Brownjohn, Modern facilities for experimental measurement of dynamic loads induced by humans: a literature review, Shock Vib. 20 (1) (2013) 53–67.
[29] R.W. Clough, J. Penzien, Dynamics of Structures, second ed., McGraw-Hill, New York, 1993.
[30] R. Sachse, The Influence of Human Occupants on the Dynamic Properties of Slender Structures (PhD Thesis), University of Sheffield, Sheffield, UK, 2002.
[31] Y. Matsumoto, M.J. Griffin, dynamic response of the standing human body exposed to vertical vibration: influence of posture and vibration magnitude, J. Sound Vib. 212 (1) (1998) 85–107.
[32] J. He, Z.F. Fu, Modal Analysis, Butterworth-Heinemann, 2001.
[33] V. Grimm, U. Berger, F. Bastiansen, S. Eliassen, V. Ginot, J. Giske, J. Goss-Custard, T. Grand, S.K. Heinz, G. Huse, A. Huth, J.U. Jepsen, C. Jørgensen, W.M. Mooij, B. Muller, G. Pe'er, C. Piou, S.F. Railsback, A.M. Robbins, M.M. Robbins, E. Rossmanith, N. Ruger, E. Strand, S. Souissi, R.A. Stillman, R. Vabo, U. Visser, D.L. DeAngelis, A standard protocol for describing individual-based and agent-based models, Ecol. Model. 198 (1–2) (2006) 115–126.
[34] Y. Miyamori, T. Obata, T. Hayashikawa, K. Sato, K. Study on identification of human walking model based on dynamic response characteristics of pedestrian bridges, in: Proceedings of the Eighth East Asia-Pacific Conference on Structural Engineering & Construction (EASEC-8), Singapore, 2001.
[35] R. Sachse, A. Pavic, P. Reynolds, The Influence of a group of human occupants on modal properties of a prototype assembly structure, in: Proceeding of the 5th European Conference on Dynamics EURODYN, 2002, pp. 1241–1246.
[36] R. Sachse, A. Pavic, P. Reynolds, Human-structure dynamic interaction in civil engineering dynamics: a literature review, Shock Vib. Digest 35 (1) (2003) 3–18, ISSN 0583-1024.
[37] J. Pfanzagl, Parametric Statistical Theory, Walter de Gruyter, Berlin, 1994, ISBN: 978-3-11-088976-5.
[38] E. Shahabpoor, A. Pavić, V. Racic, Structural vibration serviceability: new design framework featuring human-structure interaction, Eng. Struct. 136 (2017) 295–311, https://doi.org/10.1016/j.engstruct.2017.01.030.